LAWRENCE
LIVERMORE
NATIONAL
LABORATORY

LLNL-JRNL-682337

ENSO Strongly Influences Old-Growth Forest Carbon Exchange: 1998-2013 CO2 Fluxes at Wind River

S. Wharton, M. Falk

February 9, 2016

Environmental Research Letters

Disclaimer

Climate Indices Strongly Influence Old-Growth Forest Carbon Exchange

Sonia Wharton[1,*] and Matthias Falk[2]

[1]Atmospheric, Earth and Energy Division, Lawrence Livermore National Laboratory, 7000 East Avenue, L-103, Livermore, California 94550,

[2]Department of Land, Air and Water Resources, University of California, Davis, California, 95616

*Corresponding author: wharton4@llnl.gov, voice +011 925-422-9295, fax +011 925-422-5844

Short title: Climate indices influence old-growth carbon exchange

Keywords: AmeriFlux, Pacific teleconnections, ENSO, PDO, PNA, eddy covariance, biometric, interannual variability, net ecosystem exchange, old-growth

Abstract

We present a decade and a half (1998-2013) of carbon dioxide fluxes from an old-growth stand in the American Pacific Northwest to identify ecosystem-level responses to Pacific teleconnection patterns, including the El Niño/Southern Oscillation (ENSO). This study provides the longest, continuous record of old-growth eddy flux data to date from one of the longest running Fluxnet stations in the world. From 1998-2013, average annual net ecosystem exchange (F_{NEE}) at Wind River AmeriFlux was - 32 ± 84 g C m^{-2} yr^{-1} indicating that the late seral forest is on average a small net sink of atmospheric carbon. However, interannual variability is high (> 300 g C m^{-2} yr^{-1}) and shows that the stand switches from net carbon sink to source in response to climate drivers associated with ENSO. The old-growth forest is a much stronger sink during La Niña years (mean F_{NEE} = - 90 g C m^{-2} yr^{-1}) than during El Niño when the stand turns carbon neutral or into a small net carbon source (mean F_{NEE} = + 17 g C m^{-2} yr^{-1}). Forest inventory data dating back to the 1930's show a similar correlation with the lower frequency Pacific North American (PNA) and Pacific Decadal Oscillation (PDO) whereby higher aboveground net primary productivity (F_{ANPP}) is associated with cool phases of both the PNA and PDO. These measurements add evidence that carbon exchange in old-growth stands may be more sensitive to climate variability across shorter time scales than once thought.

1. Introduction

Old-growth forests represent a small fraction of western North America; in fact, only about 1.1 million hectares or 10% of their historic range exists today (Franklin and Spies 1991). While these late seral stands cover a relatively small fraction of land, they represent a significant pool of carbon that has been stored for centuries in the soil, aboveground biomass, and woody debris. This large carbon pool has the potential to be released suddenly into the atmosphere after a disturbance event, such as a forest fire, or more slowly under rising global atmospheric temperatures via increased decomposition. Without external change, however, it had been assumed that mortality and respiration balance growth in late seral forests making them carbon neutral (Odum 1965, 1969, Franklin et al. 1981). A number of recent ecosystem carbon studies (Hollinger et al. 1994, Anthoni et al. 2002, Knohl et al. 2003, Loescher et al. 2003, Desai et al. 2005, Falk et al. 2008, Luyssaert et al. 2008, Hudiburg et al. 2009, Lichstein et al. 2009, Tan et al. 2011, Wharton et al. 2012) however have put this ecological paradigm into question. For example, old-growth forests have the potential to sequester carbon at high rates (> 300 g C m^{-2} yr^{-1}) similar to younger forests if climatic conditions are favorable. This behavior has been observed in old-growth stands both in the American tropics (Loescher et al. 2003) and along the temperate American West Coast (Falk et al. 2008, Wharton et al. 2012).

Forests along the western coast of North America are subject to variations in climate via the eastward movement of weather patterns caused by equatorial and extratropical ocean-atmospheric oscillations over the Pacific Ocean (Mote et al. 2003). These correlations between distant oscillation events and local climate are called teleconnections. In the western Americas, major teleconnection events occur during strong warm and cool phases of the Pacific Decadal Oscillation (PDO), Pacific/North American Oscillation (PNA), and the El Niño-Southern Oscillation (ENSO). Cool phases of each usually bring cooler, wetter winter weather to the Pacific Northwest for time periods lasting from years (ENSO) to a decade (PNA) or multiple decades (PDO).

The interannual variability associated with ENSO has made it possible to robustly study its impacts on net ecosystem carbon exchange (F_{NEE}) in U.S. West Coast stands (Goldstein et al. 2000, Morgenstern et al. 2004, Schwalm et al. 2007) and elsewhere (e.g., Loescher et al. 2003, Schwalm et al. 2011, Parazoo et al. 2015) as flux tower records are long enough now to extend one or two decades so that they can contain multiple El Niño and La Niña events. Lower frequency oscillations such as the PDO and PNA have also been linked to eddy covariance (EC) CO_2 flux variability (e.g. Thorne and Arain 2015, Wharton et al. 2009a, Zhang et al. 2011); however, the robustness of these findings is limited by the lack of multiple events at even the longest running flux tower sites. Sites with biometric measurements, however, can have much longer measurement records (e.g., > 50 years) spanning multiple major PNA or PDO cycles.

Here, we present an unparalleled record of ecosystem carbon measurements at the oldest forest in the Fluxnet network, including fifteen years (1998-2013) of EC measurements and nearly sixty years (1948-2004) of biometric measurements at the Wind River old-growth conifer forest in southern Washington, USA. Our EC record was long enough to capture six major ENSO phase events including a strong El Niño in 1997-1998, moderate La Niña from 1998-2000, moderate El Niño in 2002-2003, moderate La Niña in 2007-2008, strong El Niño in 2009-2010, and strong La Niña in 2010-2011. To the authors knowledge this paper presents the longest ENSO-F_{NEE} analysis published to date. The biometric data captured PNA phase changes arounds 1958, 1970, 1977, 1988, and 1998, a major shift in the PDO in 1976-1977, and a second less certain PDO shift in the mid 1990's. The extended years of EC and biometric data build and advance earlier teleconnection findings at this site (Wharton et al. 2009a, Wharton et al. 2012) and show the utility of long term carbon measurement studies in assessing the response of long-living ecosystems, such as natural old forests, to climate fluctuations which occur across a wide range of time scales.

The major goals of this paper were to:

1. Identify any correlations between the Pacific climate indices and variability observed in climatic records of air temperature and precipitation at Wind River.

2. Assess whether the Wind River old-growth forest has been a stable net carbon sink, source, or carbon neutral based on eddy covariance measurements over the last fifteen years. If interannual variability is found to be significant, identify any correlations between ENSO-related climate variability (e.g., precipitation, air temperature) and annual or seasonal ecosystem flux variability (e.g., F_{NEE}, gross primary productivity, F_{GPP}, and ecosystem respiration, F_{Reco}).

3. Assess whether biometric measurements of aboveground net primary productivity at Wind River correlate with observed variability in the lower frequency Pacific oscillations, PNA and PDO.

2. Methods

2.1 Site Description

The Wind River Field Station (formerly the Wind River Canopy Crane Research Facility) is located in an unmanaged, 500-hectare, old-growth evergreen needleleaf forest in southern Washington State, USA (45° 49' 13.76" N; 121° 57' 06.88" W, 371 m above sea level). Stand characteristics are briefly given here while Shaw et al. (2004) provide a detailed ecological description.

Stand density is approximately 427 trees per hectare, tree ages range from 0 to ~500 years (Shaw et al. 2004), and leaf area index (LAI) measurements range from 8.2 to 9.2 $m^2\ m^{-2}$ with little seasonality (Thomas & Winner 2000, Roberts et al. 2004, Parker et al. 2002). The stand is dominated by evergreen conifer species including Douglas-fir (*Pseudotsuga menziesii* (Mirbel) Franco), the oldest and largest trees in diameter and height, and western hemlock (*Tsuga heterophylla* (Raf.) Sarg). Average tree heights are 52 m for Douglas-fir and 19 m for western hemlock (Ishii et al. 2000). Total estimated biomass is 619 Mg C ha^{-1}, of which 398 Mg C ha^{-1} is stored in live biomass and 221 Mg C ha^{-1} in soil and coarse and fine woody debris (Harmon et al. 2004).

2.2 Climate data

Continuous meteorological records are available for the last century from the nearby USFS Wind River Ranger Station (1919-1977) (45º 28' 47" N, 121º 33' 36" W, 351.1 m a.s.l) and Carson Fish Hatchery NOAA weather station (1977-2015) (45º 31' 12" N, 121º 34' 48" W, 345.6 m a.s.l). Historical mean annual air temperature is 8.8 ºC and mean total water-year (October-September) precipitation is 2325 mm. Precipitation is highly seasonal and is best described by water-year instead of calendar year. The forest receives more than 2 m of precipitation on average during the water-year but less than 15% usually falls during the warmest summer months when water demand is the highest.

Periods of anomalous precipitation were identified using the standardized precipitation index (SPI) (McKee et al. 1993). Positive SPI values indicate above normal precipitation while negative SPI values indicate below normal. By definition, the SPI ranges from -3 (extremely dry) to +3 (extremely wet). We calculated a 6-month SPI using the 1919-2013 precipitation record to identify seasonal precipitation anomalies that may reflect anomalies in soil reservoir storage.

Interannual and decadal climate variability in the region is driven in part by the presence and magnitude of interrelated equatorial and extratropical ocean-atmospheric oscillations, including the PDO (20-30 year cycle) (Mantua et al. 1997), PNA (~10 year cycle) (Wallace and Gutzler 1981), and ENSO (2-7 year cycle) (Wolter and Timlin 1998). Positive phases of the PDO, PNA, and Multivariate ENSO index (MEI) bring significantly warmer and drier winters to the region while negative phases bring cooler and wetter conditions (Mote et al. 2003). While all three oscillations affect the local climate, this paper focuses first on the role of ENSO. ENSO had multiple phase shifts within the fifteen year flux record which allows us to assess its influence on old-growth land surface-atmospheric carbon exchange. The influence of the PDO and PNA are considered at the end of the paper when the long-term biometric record of above-ground net primary productivity is shown for last six decades.

2.3 Ecosystem carbon data

2.3.1 Biometric

The old-growth forest has 40 ha of permanent measurement plots in nine parallel belt transects. These plots were established in 1947 and are re-measured approximately every five years to gather data on tree recruitment, growth, and mortality. Average Aboveground Net Primary Productivity (F_{ANPP}) (g C m^{-2} y^{-1}) is calculated as the mean change in live woody tree carbon storage plus tree mortality and recruitment over the re-measurement interval following methods in Harmon et al. (2004). Here, F_{ANPP} does not include biomass changes due to foliar production nor does it include heterotrophic respiration fluxes, belowground autotrophic respiration, or belowground carbon storage (e.g., changes in root biomass).

2.3.2 Micrometeorological

A full suite of half-hourly micrometeorological measurements have been taken at Wind River since 1998, including multiple heights of air temperature, relative humidity, and radiation, and multiple depths of soil temperature and soil moisture. Ecosystem flux measurements are taken above the canopy using the eddy covariance method. Net ecosystem fluxes of CO_2 (F_{NEE}) are integrated across half-hours to obtain daily, monthly and annual sums, and include the canopy storage flux term (F_s) as well as the direct eddy covariance measurement (F_c). The flux measurements are quality controlled to identify and flag periods of heavy precipitation, fog, tower shadowing, insufficient fetch, and insufficient turbulence. All missing and excluded carbon fluxes were gap-filled using algorithms devised by Reichstein et al. 2005. The ustar correction method was used to identify and "correct" nighttime carbon fluxes taken during low turbulence conditions. Ecosystem respiration fluxes (F_{Reco}) were calculated based on an empirical relationship between nighttime F_{NEE}, taken during sufficient turbulence conditions, and soil temperature and moisture. Photosynthesis (or gross primary production, F_{GPP}) was calculated as the difference between F_{NEE} and F_{Reco}. F_{Reco} and F_{GPP} are always assigned positive values such that if F_{NEE} is negative, carbon uptake by photosynthesis is greater than carbon loss by ecosystem respiration. For complete details on these

measurements and processing techniques see Paw U et al. 2004, Falk et al. 2005, Falk et al. 2008 and Wharton et al. 2012.

3. Results and Discussion

Compared to the historical climate record, the old-growth forest over the last fifteen years has, on average, experienced drier and near normal air temperature conditions. Within this long-term trend, however, is a large amount of seasonal and interannual variability spanning the full range of climate variability observed over the last century. Important seasonal anomalies include a warm winter in 2003, cool spring in 2008, 2011 and 2012, warm summer in 1998, 2003, and 2009, dry summer in 2002, 2006, and 2012, wet summer 2004, dry spring in 2007, dry winter in 2001, 2005, and 2013, and wet winter in 1999 (Figure 1). 2000-2001 had the lowest measurable precipitation since records began in 1919, while 1998-1999 was in the upper 20th percentile of historically wettest years. Some years experienced precipitation that fell more or less evenly throughout the year (2001, 2005, 2013), while in other years, the vast majority of precipitation (> 70%) came during the winter months (1999, 2000, 2002, 2006, 2007). Other years experienced relatively wet springs (2003, 2011, 2012). Most years experienced a very pronounced dry season during the summer which began, on average, in late June to early July and ended in late September to mid-October.

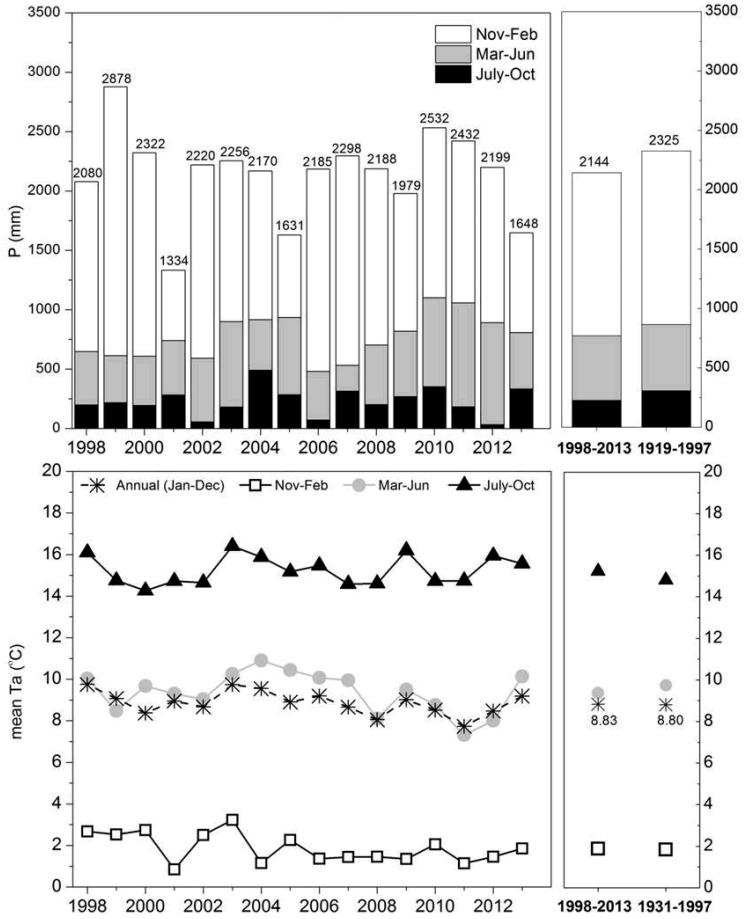

Figure 1. Seasonal total precipitation (top panel) and mean air temperature (bottom panel) for each of the flux measurements years. Average historical conditions are shown for comparison. Interannual and interseasonal variability has been high since 1998: total water-year precipitation has ranged from 2878 mm in 1999 to 1334 mm in 2001, annual mean temperature from 7.7 °C in 2011 to 9.8 °C in 1998.

A Fast Fourier Transform (FFT) was performed on the historical climate records using the statistical software package Origin 8.6 (OriginLab Corp., Northampton, MA). Power peaked at frequencies corresponding to 2.6, 11.7, and 23.5 water-years in the 1919-2013 precipitation record and 4.8 and 27.6 years in the 1930-2013 air temperature record (Figure 2). The peaks at 2.6 and 4.8 years overlap with the

average phase length for ENSO, the 11.7 years peak corresponds to the PNA, and the 23.5 and 27.6 years peaks correspond with the PDO.

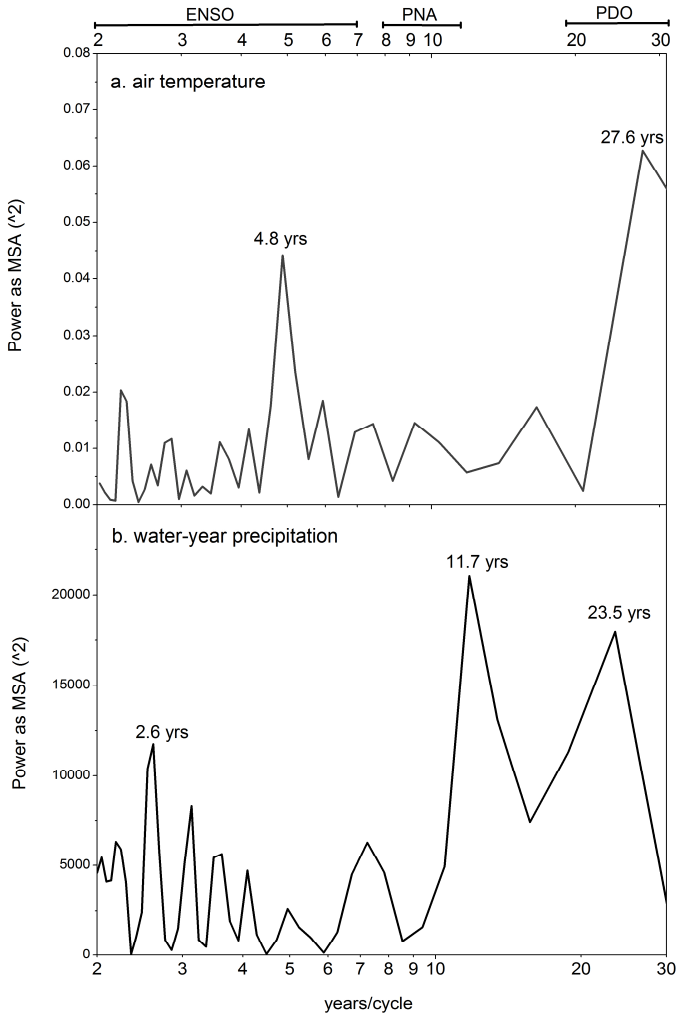

Figure 2. Fast Fourier Transform (FFT) of (a) 1930-2013 air temperature and (b) 1919-2013 water-year precipitation at Wind River shows spectral peaks corresponding to the average phase length for ENSO, PNA and PDO. Power is plotted as the mean squared amplitude (MSA) and a Hamming window was applied to the data. Note that the x-axis is plotted on the log scale.

Year-to-year variability in net ecosystem carbon exchange has been high since eddy covariance measurements began in 1998 (Figure 3). Years with significant F_{NEE} anomalies (F_{NEE} > mean F_{NEE} ± one standard deviation or - 32 ± 84 g C m^{-2} yr^{-1}) include 1999 (larger sink year), 2003 (larger source year), and 2013 (larger source year). A continuous stretch of strong net carbon uptake occurred from 2006-2008 and coincided with above normal precipitation (see Figure 1). Except for 2011, the last five years (2009-2013) have been a smaller net carbon sink than average.

On average, annual gross primary productivity (15-yr mean F_{GPP} = 1384 g C m^{-2} yr^{-1}) at Wind River is slightly larger than annual ecosystem respiration (15-yr mean F_{Reco} = 1352 g C m^{-2} yr^{-1}). The strongest net carbon sink years (F_{NEE} < - 100 g C m^{-2} yr^{-1}) included 1999, 2006, and 2008 and were driven by greater than average F_{GPP} (mean F_{GPP} = 1440 g C m^{-2} yr^{-1}) and less than average respiration (mean F_{Reco} = 1292 g C m^{-2} yr^{-1}). Strong source years were largely driven by higher rates of respiration than average (mean F_{Reco} = 1596 g C m^{-2} yr^{-1}).

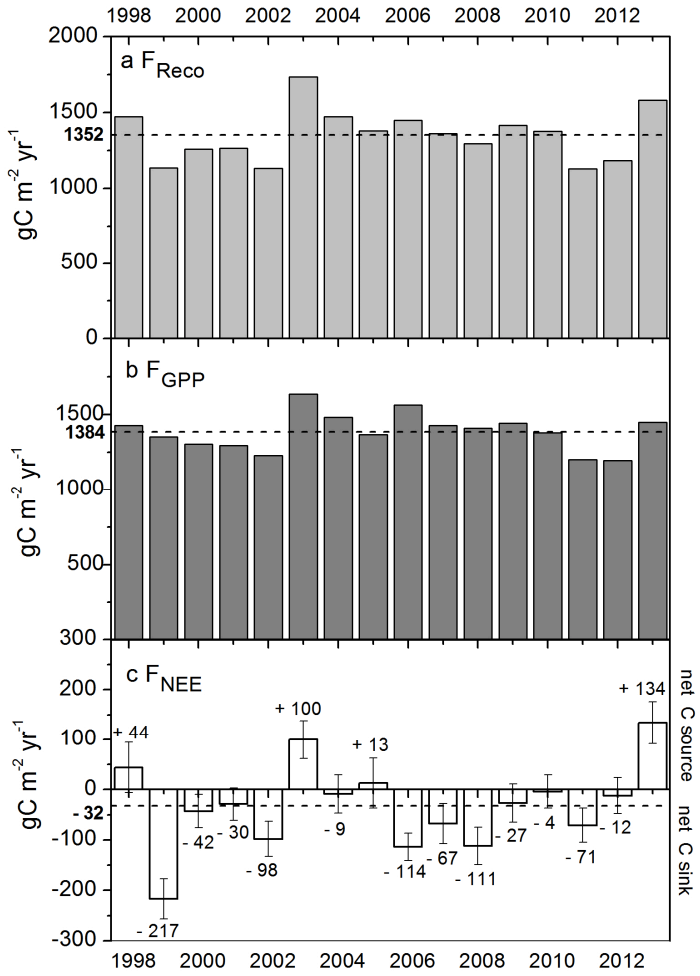

Figure 3. Year to year variability in ecosystem carbon fluxes, including (a) ecosystem respiration (F_{Reco}), (b) gross primary productivity (F_{GPP}), and (c) net ecosystem carbon exchange (F_{NEE}) over the last fifteen years. Dotted horizontal lines show the 15-year mean. Error bars on F_{NEE} include all quantifiable systematic and random errors (see Wharton et al. 2012 for methodology).

The power spectra in Figure 2 confirmed that air temperature and precipitation variability is associated with time periods corresponding to phase lengths of ENSO, PNA and PDO. To examine this relationship more closely, mean annual air temperature and winter season standardized precipitation index (SPI) were compared to the winter season Multivariate ENSO Index (MEI). Figure 4 shows that both air temperature and the SPI are moderately correlated with the winter MEI. A stronger correlation (r = 0.62) between air

temperature and MEI was found, whereby warm phases of ENSO are correlated with warmer than average annual temperatures (e.g., 1998, 2003) (Figure 4a). While the correlation (r = -0.33) between precipitation and MEI was smaller, a relationship between warm-phase ENSO and drier than normal conditions is also apparent (e.g., 2003) (Figure 4b).

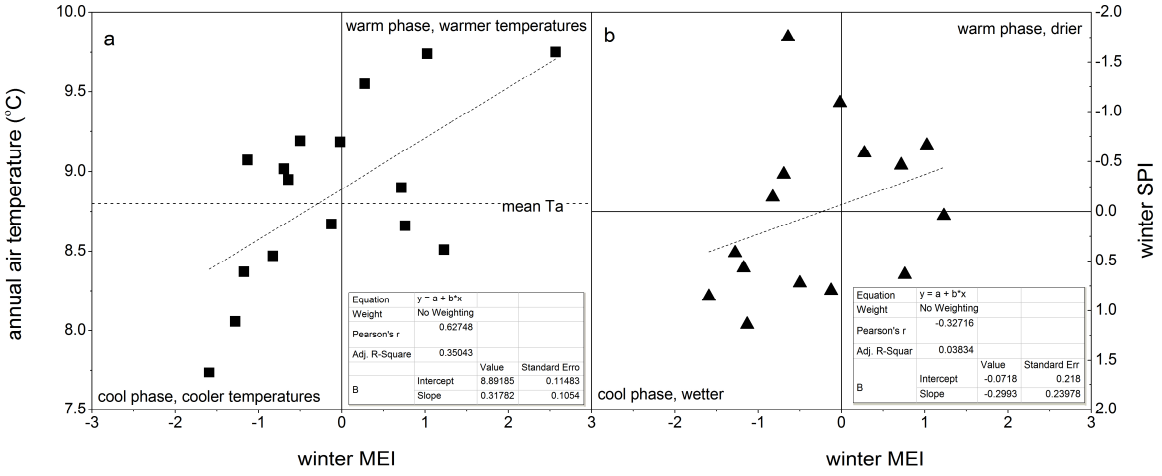

Figure 4. Linear regressions between (a) mean annual air temperature and winter multivariate ENSO index (MEI), and (b) mean October-April standardized precipitation index (SPI) and MEI. These plots show a moderate correlation between ENSO and the local climate, manifested through changes in annual temperature and winter season precipitation.

Annual F_{NEE} was next plotted against the MEI to assess if a correlation between ENSO and forest carbon sink/source strength has also existed over the last fifteen years. First, it is apparent that the source or sink strength of the old-growth forest is clearly correlated (r = -0.73) with the winter SPI. Drier than normal winters are moderately correlated with small sink years (e.g., 2001), carbon-neutral years (e.g., 2004, 2005, and 2009), or source years (e.g., 2003, 2013) (Figure 5a), while wetter winters coincide with larger sink years (e.g., 1999, 2006). A smaller, but still moderate correlation (r = 0.55) is also found when annual F_{NEE} is plotted against the winter MEI. Cool phases of ENSO are correlated with larger than

normal carbon sink years (e.g., 1999, 2008, and 2011). Likewise warm ENSO phases are correlated with carbon-neutral (e.g., 2005, 2010) or source years (e.g., 1998, 2003) (Figure 5b).

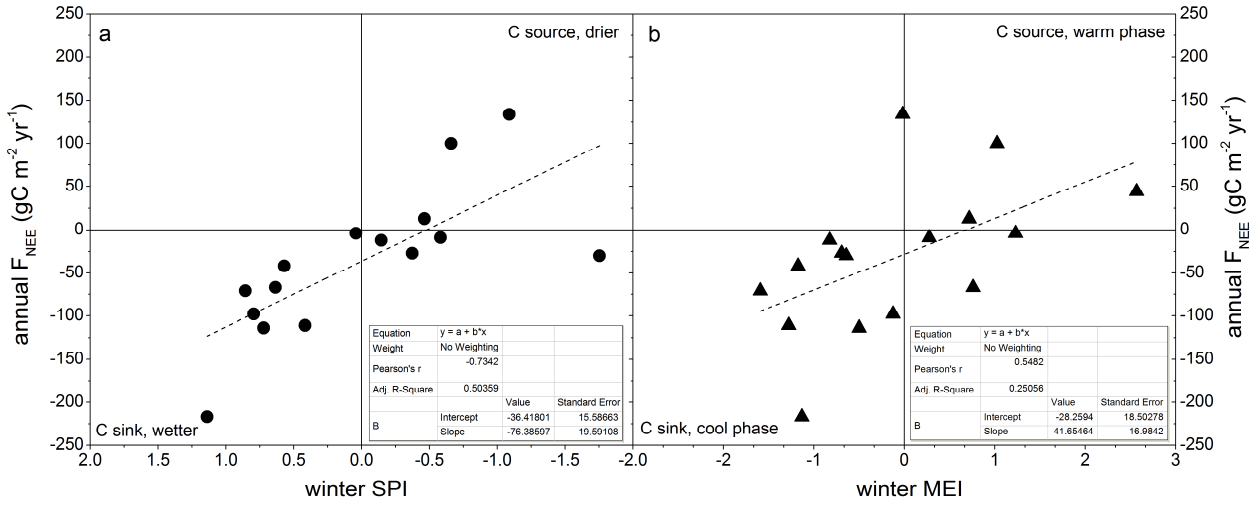

Figure 5. Linear regressions between (a) mean annual net ecosystem exchange and October-April Standardized Precipitation Index, and (b) mean annual net ecosystem exchange and winter Multivariate ENSO Index. These plots show a moderate correlation between annual net carbon exchange and winter precipitation and the MEI. Larger net carbon sink years are associated with cooler phases of ENSO and wetter winter conditions.

Environmental drivers linked to precipitation and air temperature include soil water availability, atmospheric water vapor pressure deficit (δe), photosynthetically active radiation (Q_p), and amount and type of clouds. δe is an important driver of canopy gas-atmosphere exchange because it influences stomatal conductance and can limit photosynthetic CO_2 uptake at high levels, particularly when soil moisture is limited. The F_{NEE} record at Wind River indicates that maximum half-hourly F_{NEE} uptake occurs, on average, around 12 °C and quickly declines once mean air temperatures and δe reach 20 °C and 2.0 kPa, respectively (Wagle et al. in review). Net C uptake can occur even at very low temperatures (0-5 °C) given that there is sufficient light for photosynthesis (Q_p > 50 MJ m^{-2} mo^{-1}) (Falk et al. 2005).

Figure 6 highlights the 15-yr averages for some of these environmental drivers and ecosystem fluxes. In Figure 6b, Point 1 shows the average ecological transition from net carbon source to net carbon sink in the early spring as light levels increase, atmospheric water demand is relatively low and soil moisture is plentiful. Point 2 shows the transition from net carbon sink to source in the middle of summer when water demand peaks and soil water availability becomes limiting. Note the asymmetric timing of the peaks in F_{GPP} and F_{Reco} which results in maximum cumulative net carbon uptake occurring usually in early June. Point 3 shows the region where light levels have high control over $F_{NEE,}$ microclimate conditions favor carbon uptake, and F_{GPP} reaches its annual peak. Point 4 shows the region where atmospheric water demand (and limited available soil moisture) largely limits F_{GPP} and subsequently the old-growth forest turns into a net source of carbon to the atmosphere for the rest of the year until Point 1 is reached the following winter.

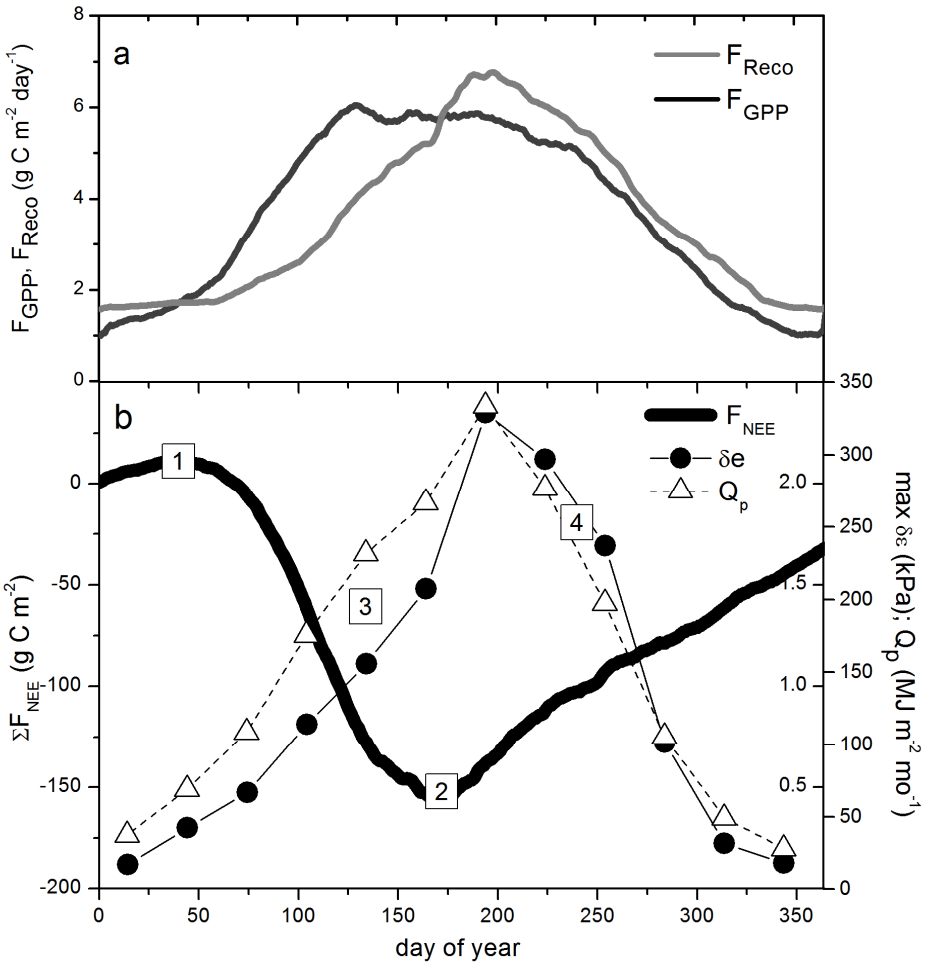

Figure 6. 15-yr average (a) daily F_{GPP}, F_{Reco} and (b) cumulative daily F_{NEE}, monthly mean maximum water vapor pressure deficit, and monthly total light levels at Wind River. Points 1-4 are described in the text.

Interannual F_{NEE} differences begin to occur, on average, between day 100-150 (mid-April-end of May) and the deviation from average continues to increase throughout the rest of the year for warm and cool ENSO phase years (Figure 7). Most years begin net carbon uptake around the same time (day 70-79, mid-March) except for cool phase years which on average start net uptake about 2-3 weeks earlier (day 56, end of February). Warm phase years end net carbon uptake on average earlier (day 148, end of May) than neutral or cool phase years (day 169-175, mid to late June).

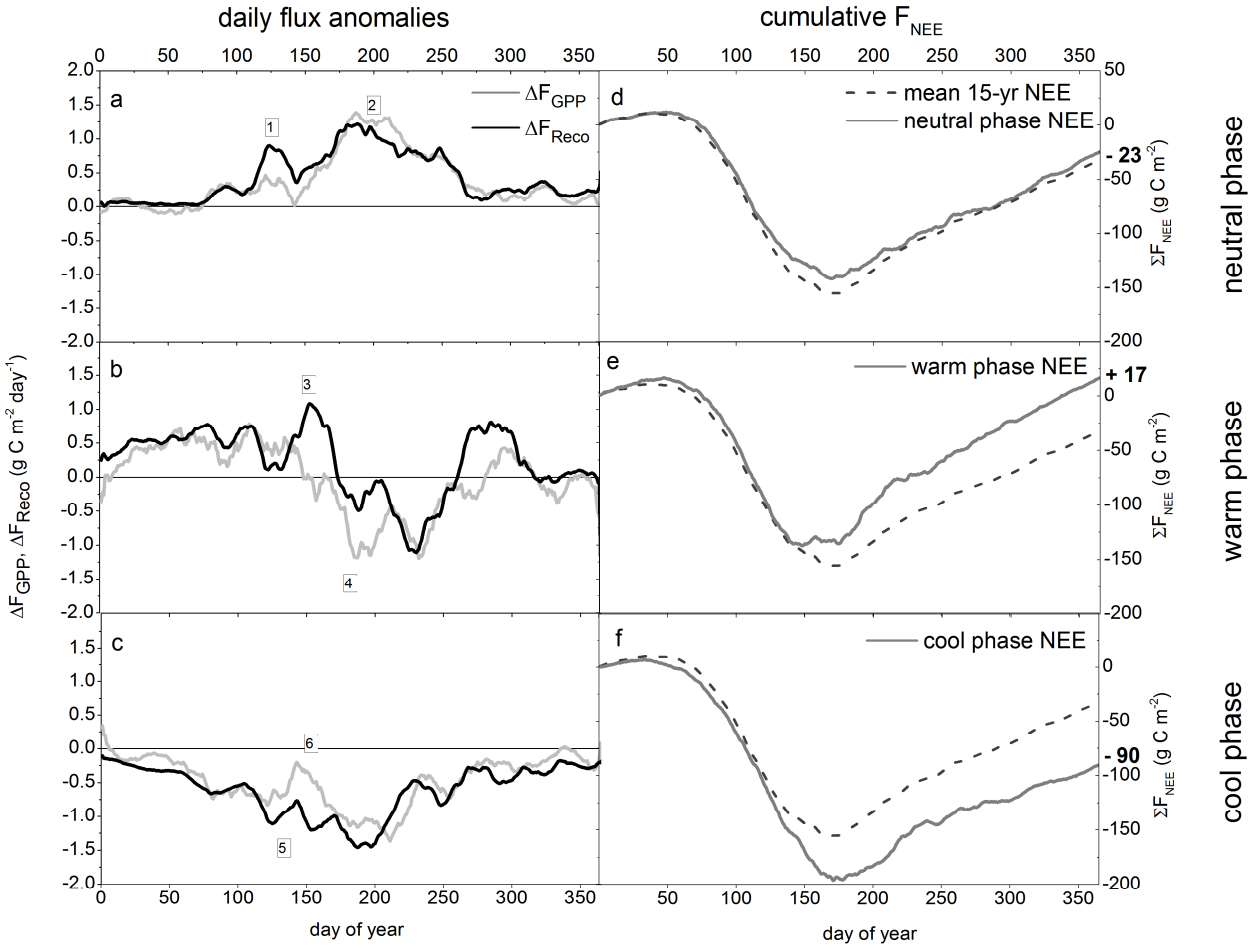

Figure 7. (a, b, c) Deviation in daily F_{GPP} and F_{Reco} from the 15-yr mean segregated by ENSO phase and (d, e, f) cumulative F_{NEE} according to ENSO phase compared to the 15-year mean. The data were smoothed with a 20pt adjacent averaging filter. Points 1-6 are described in the text.

Continuous net carbon uptake lasts on average 105 days at Wind River but this length depends on ENSO phase strength. Warm phase years see the shortest period of net uptake (70 days) while cool phase years have the longest period of continuous daily $-F_{NEE}$ (115 days). Wind River's net carbon uptake period is relatively short compared to other US evergreen forests (mean = 266 days, n = 9 forests, stand ages range from 22-110 years, mean age = 70 years) (Wagle et al. in review). The shorter net uptake period is due to a combination of geography and climate, and forest age and height. Unique site factors that limit F_{GPP}

include dry, warm summers with high atmospheric water demand, tall tree heights which induce stomatal closure even at moderate δe levels, and relatively low northern latitude winter/early spring light levels. The presence of large soil and woody biomass/debris carbon pools favor high R_{eco}.

Our carbon flux measurements show that the strongest interannual carbon flux anomalies largely occur during spring and summer months and appear to be related to ENSO climate variability. Important interannual anomalies in F_{GPP} and F_{Reco} are shown by the numbered points in Figures 7a-c. Point 1 shows that during neutral phase years, F_{Reco} is higher than normal in the spring and is greater than F_{GPP} anomalies. Point 2 shows that neutral year summer months have larger F_{GPP} anomalies than F_{Reco} and F_{GPP} is higher than the 15-year mean. These deviations cause average annual F_{NEE} during neutral years to be very close to the 15-year mean.

During warm phase years, Point 3 shows that F_{Reco} is much higher than normal in the spring/early summer due to warmer temperatures while F_{GPP} anomalies are near normal. Although note that by mid-summer (Point 4), F_{GPP} significantly decreases compared to the 15-year mean due to higher water stress. Past work has shown that the upper canopy Douglas-fir foliage is largely driving observed variability in ecosystem carbon exchange at the old-growth forest (Wharton et al. 2009b). When δe is moderate or high and soil moisture is limiting stomatal conductance in these tall trees sharply declines before midday which greatly limits F_{GPP} (Ryan and Yoder 1997, Wharton et al. 2009b). By late summer F_{Reco} has also significantly decreased compared to normal due to low soil moisture availability and is perhaps driven by a reduction in root respiration rates. Root respiration at Wind River has been shown to decrease during drier periods (Taylor et al. 2015). Overall mean annual F_{NEE} during warm phase years shows that the forest acts as a small carbon source.

During cool phase years both F_{GPP} and F_{Reco} are attenuated in the late spring due to lower temperatures although reductions in F_{Reco} are slightly larger (Point 5) leading to greater net carbon uptake than normal.

By early June, Point 6, F_{Reco} stays strongly attenuated due to lower temperatures in the canopy while F_{GPP} moves closer to normal conditions. Both points 5 and 6 favor net carbon uptake and the forest acts as a moderate net carbon sink during cool-phase ENSO years.

Attributing anomalies in F_{NEE} to specific environmental drivers is confounded by the fact that the different ecosystem processes which determine respiration and photosynthesis are correlated with climate variables across a wide range of time scales. Wavelet cospectra analysis provides some insights into these complex relationships. A recent study by Wagle et al. (in review) has shown that Wind River F_{NEE} and Q_p are most highly correlated on daily time scales, F_{NEE} and δe on weekly and monthly scales, F_{NEE} and Ta on seasonal time scales, and F_{NEE} and soil moisture on interannual time scales. This analysis also showed that drivers that vary seasonally or annually were more important for F_{NEE} in semi-arid and Mediterranean sites, including Wind River, than in locations with evenly distributed precipitation. Larger variability in F_{NEE} in semi-arid and Mediterranean sites at longer timescales might be related to larger year-to-year variability in soil water availability and drought duration, and the length of cumulative net carbon uptake in these sites (Wagle et al. in review).

While the EC flux record at Wind River encompasses multiple phase changes in ENSO and reveals anomalies on the daily, seasonal and interannual time scales, the 60-year climatological and biometric records at the site have the lengths needed to also include multi-decadal phase changes in the PDO and PNA. These records include a major shift in the PDO in 1976-1977. At this time the PDO shifted out of a multi-decadal cool phase into a warm phase. The precipitation data at Wind River show wetter conditions (mean SPI = +0.5) during the cool PDO phase and drier conditions (mean SPI = -0.2) after the PDO switch. A less certain PDO switch to a cool phase may have occurred in the mid-1990's although the SPI data at Wind River do not show a subsequent increase in precipitation (mean SPI = -0.3).

Figure 8 shows that the PDO and PNA have been largely in-phase with the exception of the most recent five years as the PDO has been in a cool phase but the PNA has stayed weakly positive. The biometric F_{ANPP} measurements (five year averages ending in the year shown) indicate an overall decrease in F_{ANPP} since the 1950-1960's. Exceptions to this occur in 1958 and 1978 (shown as open circles in Figure 8c); both measurement years include increased mortality following significant Douglas-fir beetle tree kills in 1951 and 1973, respectively. The short period of increasing F_{ANPP} from 1960-1972 is likely due to stand recovery following the first disturbance event which created gaps in the canopy leading to increased recruitment and growth in the lower canopy. Correlations between F_{ANPP} and the PDO and PNA are shown in Figure 9. The post-disturbance F_{ANPP} measurements taken in 1958 and 1978 were removed from these plots. Higher F_{ANPP} is correlated with cooler phases of both the PNA and PDO. This finding agrees with tree ring studies in the lower Cascade forests which indicate that radial growth is limited by low summer precipitation and high summer temperatures and increases with higher winter precipitation (Case and Peterson 2005).

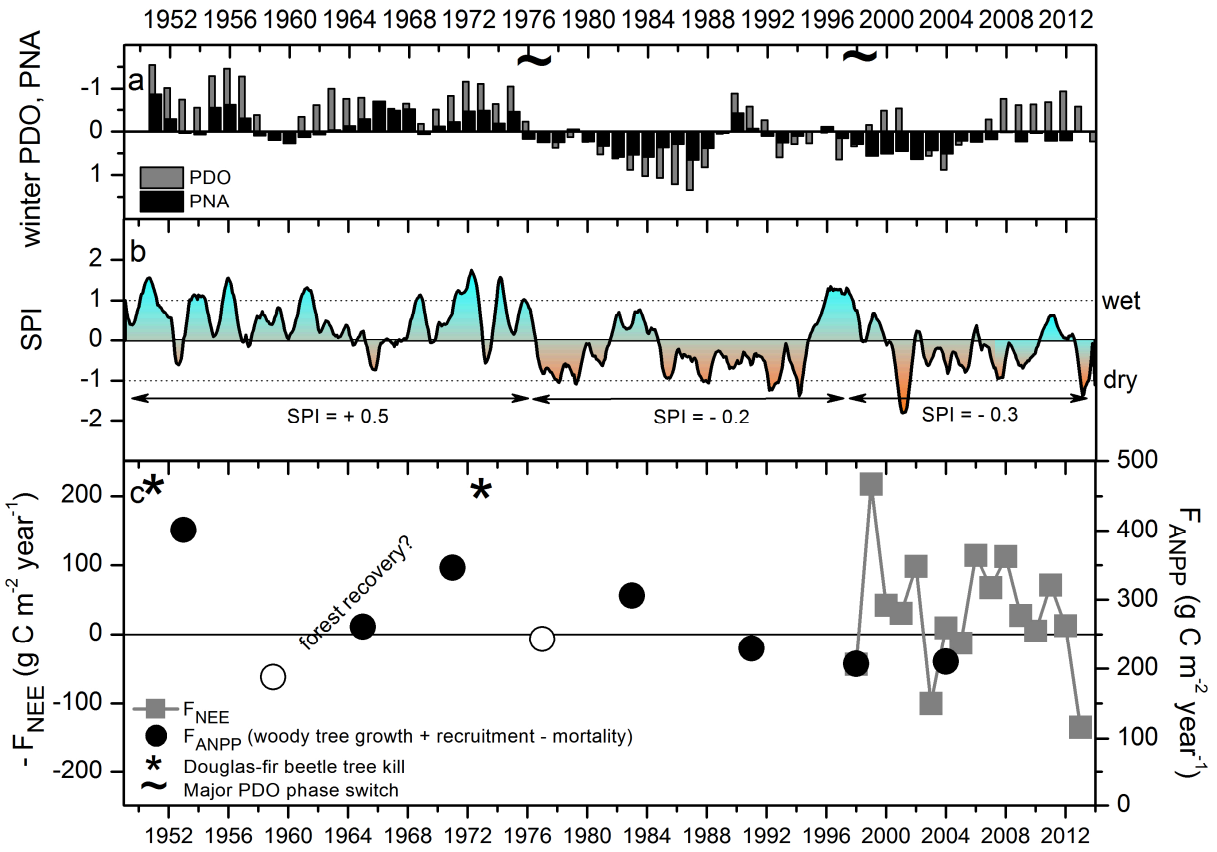

Figure 8. Time series of climate and ecosystem carbon observations with highlighted known disturbance events and climate phase shifts. Shown are (a) winter PDO and PNA with a 3pt smoothing filter, (b) 6-month SPI, and (c) mean annual aboveground net primary productivity and annual net ecosystem exchange (eddy covariance) measurements. F_{NEE} is shown as $-F_{NEE}$ to ease comparison with the other variables. The biometric measurements which contain high amounts of disturbance-induced mortality are shown as open circles.

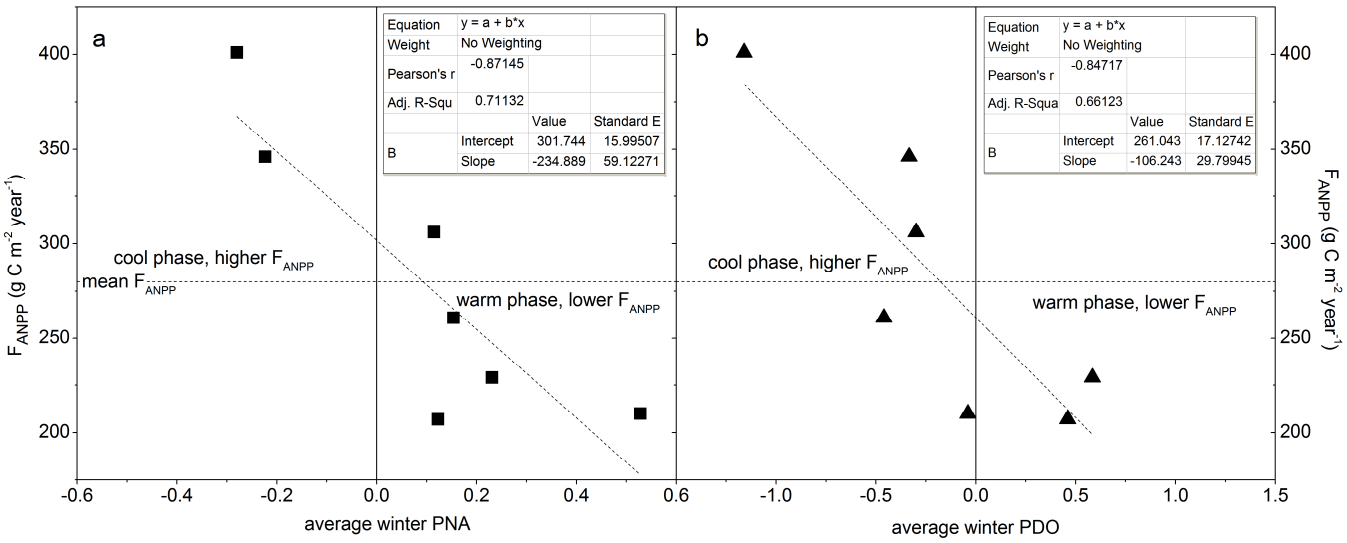

Figure 9. Linear regressions between biometic F_{ANPP} and average wintertime (a) PNA and (b) PDO. The PNA and PDO are 5-year means with time periods overlapping the F_{ANPP} measurement cycles. These plots show correlation between climate index and F_{ANPP} such that warm phase periods are associated with lower than average F_{ANPP}.

4. Conclusions

Luyssaert et al. (2008) suggest that many old-growth stands are, on average, moderate to large net sinks of atmospheric carbon (~ -200 g C m^{-2} yr^{-1}) due to the imbalance between slow decomposition of dead wood and fast recovery of living vegetation from natural gap events. At Wind River we have not observed this over the last fifteen years; instead the 500 year old forest has been a small average net carbon sink (-32 g C m^{-2} yr^{-1}). Our EC measurements are in better agreement with modeled (-49 g C m^{-2} yr^{-1}) (Turner et al. 2015) and biometric estimates (-15 g C m^{-2} yr^{-1}) (Gray et al. 2016) of other old-growth stands in the region. However, interannual variability in F_{NEE} is high at Wind River and favorable meteorological conditions during La Niña years have the potential to turn the old-growth forest into a much stronger sink as we observed significantly lower F_{Reco} during these events. The magnitude of F_{NEE} interannual variability adds evidence that old-growth forests may be more pliable to climate forcings on shorter time scales than the traditional ecological theory predicts. The sixty year record of F_{ANPP} also

shows a correlation with the two major lower frequency oscillations, the PNA and PDO, such that higher F_{ANPP} is also associated with cooler phases of both. This longer time record contained at least two major disturbance events. Confounding influences of climate-induced disturbances (e.g., insect outbreaks, fungal disease, fire) on mortality and forest growth highlight the need for both long-term (e.g., biometric forest inventory data) and short-term records (e.g., eddy covariance data) to fully assess climate phase-ecosystem interactions, as natural regeneration and biomass decomposition occur across different time scales (Luyssaert et al. 2008).

5. Acknowledgements

S.W. dedicates this manuscript to Jacqueline Wharton (1949-2015), whose encouragement of my curiosity about the natural world will not be forgotten. The authors would like to thank the staff at the Wind River Field Station for their hospitality and assistance. Special thanks go to our field technician Matt Schroeder who calibrated and maintained equipment through even the wettest of PNW winters. Gratitude goes to the former Principal Investigators Dr. Kyaw Tha Paw U at the University of California, Davis and Dr. Ken Bible at the University of Washington, Seattle. The Wind River Field Station is operated under a joint sponsorship of the University of Washington and the USDA Forest Service/PNW Station and we acknowledge both for significant support. Lawrence Livermore is operated by Lawrence Livermore National Security, LLC, for the U.S. Department of Energy, National Nuclear Security Administration under Contract DE-AC52-07NA27344. LLNL-JRNL-682337

6. References

Anthoni, P.M., Unsworth, M.H., Law, B.E., Irvine, J., Baldocchi, D.D., Van Tuyl, S., Moore, D., 2002. Seasonal differences in carbon and water vapor exchange in young and old-growth ponderosa pine ecosystems. Agric. For. Meteorol. 111, 203-222.

Desai, A.R., Bolstad, P.V., Cook, B.D., Davis, K.J., Carey, E.V., 2005. Comparing net ecosystem exchange of carbon dioxide between an old-growth and mature forest in the upper Midwest, USA. Agric. For. Meteorol. 128, 35-55.

Falk, M., Paw U, K.T., Wharton, S., Schroeder, S.M., 2005. Is soil respiration a major contributor to the carbon budget within a Pacific Northwest old-growth forest? Agric. For. Meteorol. 135, 269-283.

Falk, M., Wharton, S., Schroeder, M., Ustin, S., Paw U, K.T.., 2008. Flux partitioning in an old growth forests: seasonal and interannual dynamics. Tree Physiology 28, 509-520.

Franklin, J., F., Cromack, K., Denison, W., McKee, A., Maser, C., Sedell, J., Swanson, F., Juday, G., 1981. Ecological Characteristics of Old-Growth Douglas-fir Forests, General Technical Report PNW-118. Pacific Northwest Forest and Range Experimental Station, Portland, Oregon, 48 pp.

Franklin, J.F., Spies, T.A., 1991. Ecological definitions of old-growth Douglas-fir forests. In: Ruggiero, L.F., Aubry, K.B., Carey, A.B., Huff, M.H. (Eds.), Wildlife and Vegetation of Unmanaged Douglas-fir Forests, U.S. Department of Agriculture, Forest Service, Portland, Oregon, General Technical Report PNW-285.

Goldstein, A.H., Hultman, N.E., Fracheboud, J.M., Bauer, M.R., Panek, J.A., Xu, M., Qi, Y., Guenther, A.B., Baugh, W., 2000. Effects of climate variability on the carbon dioxide, water and sensible heat fluxes above a ponderosa pine plantation in the Sierra Nevada (CA). Agric. For. Meteorol. 101, 113-129.

Gray, A.N., Whittier, T.R., Harmon, M.E., 2016. Carbon stocks and accumulation rates in Pacific Northwest forests: role of stand age, plant community, and productivity. Ecosphere 7(1):e01224.10.1002/ecs2.1224

Harmon, M.E., Bible, K., Ryan, M.G., Shaw, D.C., Chen, H., Klopatek, J., Li, X., 2004. Production, respiration, and overall carbon balance in an old-growth *Pseudotsuga-tsuga* forest ecosystem. Ecosystems 7, 498-512.

Hollinger, D.Y., Kelliher, F.M., Byers, J.N., Hunt, J.E., McSeveny, M., Weir, P.L., 1994. Carbon dioxide exchange between an undisturbed old-growth temperate forest and the atmosphere. Ecology 75, 134-150.

Hudiburg T., Law, B.E., Turner, D.P., Campbell, J., Donato, D., Duane, M., 2009. Carbon dynamics of Oregon and Northern California forests and potential land-based carbon storage. Ecol. Appl. 19, 163-180.

Ishii, H., Reynolds, J.H., Ford, E.D., Shaw, D.C., 2000. Height growth and vertical development of an old-growth *Pseudotsuga-Tsuga* forest in southwestern Washington State, USA. Can. J. For. Res. 30, 17-24.

Knohl, A., Schulze, E.-D., Kolle. O., Buchmann, N., 2003. Large carbon uptake by an unmanaged 250-year old deciduous forest in Central Germany. Agric. For. Meteor. 118, 151-167.

Lichstein, J.W., Wirth, C., Horn, H.S., Pacala, S.W., 2009. Biomass chronosequences of United States forests: implications for carbon storage and forest management. In: Wirth, C. et al. (Eds.), Old-Growth Forests. Springer-Verlag, Berlin.

Loescher, H.W., Oberbauer, S.F., Gholz, H.L., Clark, D.B., 2003. Environmental controls on net ecosystem-level carbon exchange and productivity in a Central American tropical wet forest. Global Change Biol. 9, 396-412.

Luyssaert, S., Schulze, E.-D., Borner, A., Knohl, A., Hessenmoller, D., Law, B.E., Ciais, P., Grace, J., 2008. Old-growth forests as global carbon sinks. Nature 445, 213-215.

Mantua, N.J., Hare, S.R., Zhang, Y., Wallace, J.M., Francis, R.C., 1997. A Pacific interdecadal climate oscillation with impacts on salmon production. Bull. Amer. Meteor. Soc. 78, 1069-1079.

McKee, T.B., Doesken, N.J., Kleist, J., 1993. The relationship of drought frequency and duration to time scales. In: Eighth Conf. Appl. Climatol., Anaheim, CA, USA, 179-184.

Morgenstern, K., Black, T.A., Humphreys, E.R., Griffis, T.J., Drewitt, G.B., Cai, T., Nesic, Z., Spittlehouse, D.L., Livingston, N.J., 2004. Sensitivity and uncertainty of the carbon balance of a Pacific Northwest Douglas-fir forest during an El Niño/La Niña cycle. Agric. For. Meteorol. 123, 201-219.

Mote, P.W., Parson, E., Hamlet, A.F., Keeton, W.S., Lettenmaier, D., Mantau, N., Miles, E.L., Peterson, D., Peterson, D.L., Slaighter, R. Snover, A.K., 2003. Preparing for climatic change: the water, salmon, and forests of the Pacific Northwest. Clim. Change 61, 45-88.

Odum, E., 1965. Fundamentals of Ecology. Saunders, Philadelphia, PA, USA.

Odum, E.P., 1969. The strategy of ecosystem development. Science 164, 262-270.

Parker, G.G., Davis, M.M., Chapotin, S.M., 2002. Canopy light transmittance in Doulgas-fir-western-hemlock stands. Tree Physiol. 22, 147-157.

Parazoo, N.C., Barnes, E., Worden, J., Harper, A.B., Bowman, K.B., Frankenberg, C., Wolf, S., Litvak, M., Keenan, T.F., 2015. Influence of ENSO and the NAO on terrestrial carbon uptake in the Texas-northern Mexico region. Global Biogeo. Cycles 29, 1247-1265.

Paw U, K.T., Falk, M., Suchanek, T.H., Ustin, S.L., Chen, J., Park, Y.-S., Winner, W.E., Thomas, S.C., Hsiao, T.C., Shaw, R.H., King, T.S., Pyles, R.D., Schroeder, M., Matista, A.A., 2004. Carbon dioxide exchange between an old-growth forest and the atmosphere. Ecosystems 7, 513-524.

Reichstein, M., Falge, E., Baldocchi, D., Papale, D., Aubinet, M., Berbigier, P., Bernhofer, C., Buchmann, N., Gilmanov, T., Granier, A., Grunwald, T., Havrankova, K., Ilvesniemi, H., Janous, D., Knohl, A., Laurila, T., Lohila, A., Loustau, D., Matteucci, G., Meyers, T., Miglietta, F., Ourcival, J.-M.,

Pumpanen, J., Rambal, S., Rotenberg E., Sanz, M., Tenhunen, J., Seufert, G., Vaccari, F., Vesala, T., Yakir, D., Valentini, R., 2005. On the separation of net ecosystem exchange into assimilation and ecosystem respiration: review and improved algorithm. Global Change Biol. 11, 1424–1439.

Roberts, D.A., Ustin, S.L., Ogunjemiyo, S., Greenberg, J., Dobrowski, S.Z., Chen, J., Hinckley, T.M., 2004. Spectral and structural measures of Northwest forest vegetation at leaf to landscape scales. Ecosystems 7, 545-562.

Ryan, M.G., Yoder, B.J. 1997. Hydraulic limits to tree height and tree growth. Bioscience 47, 235-242.

Schwalm, C.R., Black, T.A., Morgenstern, K., Humphreys, E.R., 2007. A method for deriving net primary productivity and component respiration fluxes from tower-based eddy covariance data: a case study using a 17-year data record from a Douglas-fir chronosequence. Global Change Biol. 13, 370-385.

Schwalm, C.R., Williams, C.A., Schaefer, K., Baker, I., Collatz, G.J., Rodenbeck, C., 2011. Does terrestrial drought explain global CO_2 flux anomalies induced by El Niño? Biogeosciences 8, 2493-2506.

Shaw, D.C., Franklin, J.F., Bible, K., Klopatek, J., Freeman, E., Greene, S., Parker, G.G., 2004. Ecological setting of the Wind River old-growth forest. Ecosystems 7, 427-439.

Tan, Z.H., Zhang, Y.P., Schaefer, D., Yu, G.R., Liang, N.S., Song, Q.H., 2011. An old-growth subtropical Asian evergreen forest as a large carbon sink. Atmos. Environ. 45, 1548-1554.

Taylor, A.J., Lai, C.-T., Hopkins, F.M., Wharton, S., Bible, K., Xu, X., Phillips, C., Bush, S., Ehleringer, J.R., 2015. Radiocarbon-based partitioning of soil respiration in an old-growth coniferous forest. Ecosystems 18, 459-470.

Thomas, S.C., Winner, W.E., 2000. Leaf area index of an old-growth Douglas-fir forest estimated from direct structural measurements in the canopy. Can J. For. Res. 30, 1922–1930.

Thorne, R., Arain, M.A., 2015. Influence of low frequency variability on climate and carbon fluxes in a temperate pine forest in eastern Canada. Forests 6, 2762-2784.

Turner, D.P., Ritts, W.D., Kennedy, R.E., Gray, A.N., Yang, Z., 2015. Effects of harvest, fire, and pest/pathogen disturbances on the West Cascades ecoregion carbon balance. Carbon Bal. Manage. 10:12, DOI 10.1186/s13021-015-0022-9

Wagle, P., Xiao, X.-M., Kolb, T., Law, B.E., Wharton, S., Monson, R.K., Chen, J., Blanken, P.D., Novick, K.A., Dore, S., Noormets, A., Gowda, P.H. Differential responses of carbon and water vapor fluxes to climate among evergreen needleleaf forests across the United States. Ecological Processes, in review.

Wallace, J.M., Gutzler, D.S., 1981. Teleconnections in the geopotential height field during the Northern Hemispheric winter. Mon. Weath. Rev. 109, 784-812.

Wharton, S., Chasmer, L., Falk, M., Paw U, K.T., 2009a. Strong links between teleconnections and ecosystem exchange found at a Pacific Northwest old-growth forest from flux tower and MODIS EVI data. Global Change Biol. 15, 2187-2205.

Wharton, S., Schroeder, M., Bible, K., Falk, M., Paw U, K.T., 2009b. Stand-level gas-exchange responses to seasonal drought in very young versus old Douglas-fir forests of the Pacific Northwest, USA. Tree Physiol. 29, 959-974

Wharton, S., Falk, M., Bible, K., Schroeder, M., Paw U, K.T., 2012. Old-growth CO_2 flux measurements reveal high sensitivity to climate anomalies across seasonal, annual and decadal time scales. Agric. For. Meteorol. 161, 1-14.

Wolter, K., Timlin, M.S., 1998. Measuring the strength of ENSO events: how does 1997/1998 rank? Weather 53, 315-324.